Ehrlichia SLiM Ligand Mimetic Activates Notch Signaling in Human Monocytes

LaNisha L. Patterson,[a] Thangam Sudha Velayutham,[a] Caitlan D. Byerly,[a] Duc Cuong Bui,[a] Jignesh Patel,[a] Veljko Veljkovic,[f] Slobodan Paessler,[a] Jere W. McBride[a,b,c,d,e]

[a]Department of Pathology, University of Texas Medical Branch, Galveston, Texas, USA
[b]Microbiology and Immunology, University of Texas Medical Branch, Galveston, Texas, USA
[c]Center for Biodefense and Emerging Infectious Diseases, University of Texas Medical Branch, Galveston, Texas, USA
[d]Sealy Institute for Vaccine Sciences, University of Texas Medical Branch, Galveston, Texas, USA
[e]Institute for Human Infections and Immunity, University of Texas Medical Branch, Galveston, Texas, USA
[f]Biomed Protection, LLC, Galveston, Texas, USA

ABSTRACT *Ehrlichia chaffeensis* evades innate host defenses by reprogramming the mononuclear phagocyte through mechanisms that involve the exploitation of multiple evolutionarily conserved cellular signaling pathways, including Notch. This immune evasion strategy is directed in part by tandem repeat protein (TRP) effectors. Specifically, the TRP120 effector activates and regulates Notch signaling through interactions with the Notch receptor and the negative regulator, F-Box and WD repeat domain-containing 7 (FBW7). However, the specific molecular interactions and motifs required for *E. chaffeensis* TRP120-Notch receptor interaction and activation have not been defined. To investigate the molecular basis of TRP120 Notch activation, we compared TRP120 with endogenous canonical/noncanonical Notch ligands and identified a short region of sequence homology within the tandem repeat (TR) domain. TRP120 was predicted to share biological function with Notch ligands, and a function-associated sequence in the TR domain was identified. To investigate TRP120-Notch receptor interactions, colocalization between TRP120 and endogenous Notch-1 was observed. Moreover, direct interactions between full-length TRP120, the TRP120 TR domain containing the putative Notch ligand sequence, and the Notch receptor LBR were demonstrated. To molecularly define the TRP120 Notch activation motif, peptide mapping was used to identify an 11-amino acid short linear motif (SLiM) located within the TRP120 TR that activated Notch signaling and downstream gene expression. Peptide mutants of the Notch SLiM or anti-Notch SLiM antibody reduced or eliminated Notch activation and NICD nuclear translocation. This investigation reveals a novel molecularly defined pathogen encoded Notch SLiM mimetic that activates Notch signaling consistent with endogenous ligands.

IMPORTANCE *E. chaffeensis* infects and replicates in mononuclear phagocytes, but how it evades innate immune defenses of this indispensable primary innate immune cell is not well understood. This investigation revealed the molecular details of a ligand mimicry cellular reprogramming strategy that involved a short linear motif (SLiM), which enabled *E. chaffeensis* to exploit host cell signaling to establish and maintain infection. *E. chaffeensis* TRP120 is a moonlighting effector that has been associated with cellular activation and other functions, including ubiquitin ligase activity. Herein, we identified and demonstrated that a SLiM present within each tandem repeat of TRP120 activated Notch signaling. Notch is an evolutionarily conserved signaling pathway responsible for many cell functions, including cell fate, development, and innate immunity. This study is significant because it revealed the first molecularly defined pathogen encoded SLiM that appears to have evolved *de novo* to mimic endogenous Notch ligands. Understanding Notch activation during

E. chaffeensis infection provides a model to study pathogen exploitation of signaling pathways and will be useful in developing molecularly targeted countermeasures for inhibiting infection by a multitude of disease-causing pathogens that exploit cell signaling through molecular mimicry.

KEYWORDS *Ehrlichia*, Notch signaling, effector, ligand, molecular mimicry, short linear motif, tandem repeat protein

*E*hrlichia chaffeensis is a small, obligately intracellular, Gram-negative tick-transmitted bacterium (1) that exhibits tropism for mononuclear phagocytes. *E. chaffeensis* establishes infection through a multitude of cellular reprogramming strategies that involve effector-host interactions resulting in activation and manipulation of cell signaling pathways to suppress and evade innate immune mechanisms (2–8). The mechanisms whereby *E. chaffeensis* evades host defenses of the macrophage involves the exploitation of Wnt and Notch signaling by the tandem repeat protein (TRP) effector, TRP120 (2–6).

E. chaffeensis TRP120 is a surface-expressed and intracellularly secreted effector that has well-documented moonlighting functions, including roles as a nucleomodulin (9, 10), a homologous to E6AP C terminus (HECT) E3 ubiquitin ligase (2, 7, 11), and as a ligand mimic (3, 5, 6, 12). Previously, we found that TRP120 is involved in a diverse array of host cell interactions, including components of signaling and transcriptional regulation associated with Wnt and Notch signaling pathways (8). We recently showed that TRP120 ubiquitinates the Notch negative regulator FBW7 resulting in increased Notch intracellular domain (NICD) levels and other FBW7-regulated oncoproteins during infection (2). In addition, we also demonstrated that *E. chaffeensis* Notch activation resulted in downregulation of toll-like receptor 2 and 4 expressions, likely as an immune evasion mechanism (6). Although we demonstrated TRP120 activated Notch signaling, the molecular details involved in activation have yet to be defined.

The Notch signaling pathway is evolutionarily conserved and is known to play a critical role in cell proliferation, differentiation, and apoptosis in all metazoan organisms (13–16). Notch activation plays significant roles in various other cellular outcomes, including MHC Class II expansion (17), B and T cell development (18), and innate immune mechanisms, such as autophagy (19) and apoptosis (20, 21). Canonical Notch activation is driven by direct cell-membrane bound receptor-ligand interactions with four Notch receptors (Notch 1 to 4) and canonical Notch ligands, Delta-like (DLL 1, 3, and 4) and Jagged (Jagged/Serrate-1 and 2). Notch receptor-ligand interactions occur at the Notch extracellular domain (NECD), specifically at epidermal growth factor-like repeats (EGFs) 11 to 13, the known ligand-binding domain (LBD). A module at the N terminus of Notch ligands (MNNL) and Delta/Serrate/LAG-2 (DSL) domains in canonical Notch ligands interact with the Notch LBD. Although there is evidence demonstrating the requirement of both N-terminal MNNL and DSL Notch ligand domains for Notch receptor binding, there is little information known about ligand regions/motifs that are necessary for Notch activation (22, 23). During canonical Notch activation, ligands expressed on neighboring cells bind the Notch receptor and create a mechanical force at the negative regulatory region (NRR), which triggers several sequential proteolytic cleavages, releasing the NICD. NICD subsequently translocates to the nucleus and binds to other transcriptional coactivators, including RBPjK and MAML, to activate Notch gene transcription. Notably, secreted noncanonical Notch ligands have also been shown to activate Notch signaling. However, the molecular details of noncanonical Notch ligand-receptor interactions are not well defined.

There are three major classes of protein interaction modules which include globular domains, intrinsically disordered domains (IDDs), and short linear motifs (SLiMs), all of which have distinct biophysical attributes (24–26). IDDs are 20 to 50 amino acids in length, are known to be disordered, are located within globular domains or intrinsically disordered protein regions and have transient interactions in the nanomolar range. In

comparison, SLiMs are ~3 to 12 amino acids in length, are known to be disordered, located within globular domains or IDDs, and have low micromolar affinity ranges with transient interactions. SLiMs have been shown to evolve *de novo* for promiscuous binding to various partners (26, 27). Ehrlichial TRPs interact with a diverse array of host proteins through several well-known protein-protein interaction mechanisms, including posttranslational modifications (PTMs) and various protein interaction modules located in IDDs (7, 9, 26, 28).
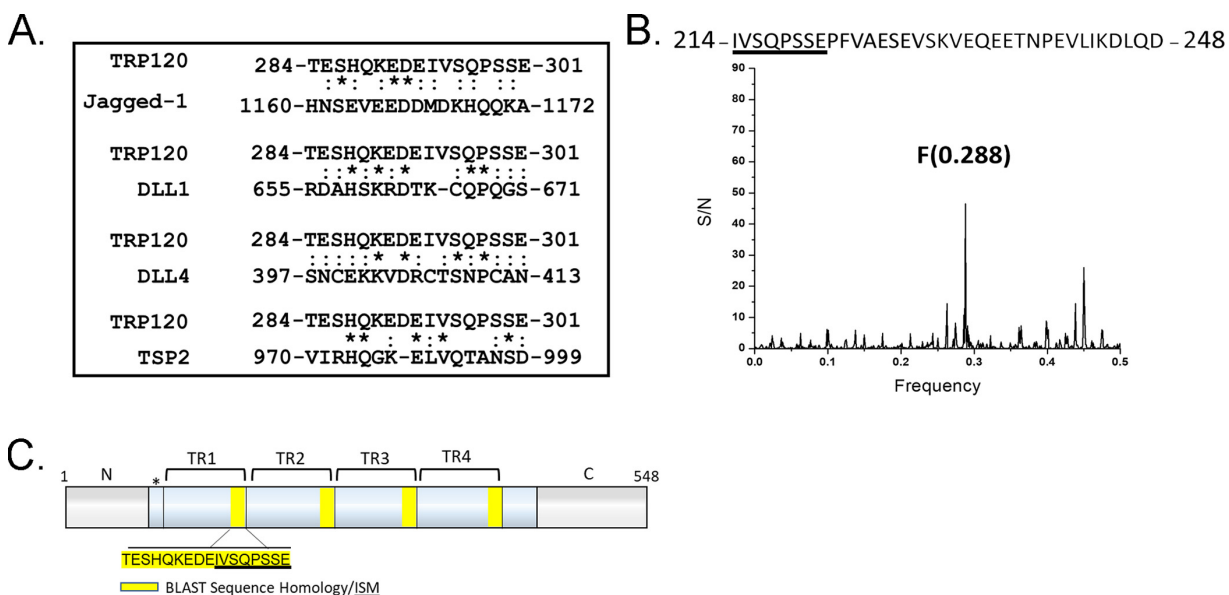
Microorganisms have developed mechanisms to survive in the host cell, which involve hijacking host cell processes. Molecular mimicry has been well-established as an evolutionary survival strategy utilized by pathogens to disrupt or coopt host function for infection and survival (26–29). Studies have determined this occurs through pathogen effectors that mimic eukaryotic host proteins, allowing for pathogens to hijack and manipulate host cellular pathways and functions. SLiMs have been identified as interaction modules whereby eukaryotes and pathogens direct cellular processes through protein-protein interactions (29, 30). Recently, we demonstrated TRP120 is a Wnt ligand mimetic that interacts with host Wnt receptors to activate Wnt signaling (3).

In this study, we revealed an *E. chaffeensis* Notch SLiM ligand mimetic whereby TRP120 activated Notch signaling for infection and intracellular survival. Understanding the molecular mechanisms utilized by *E. chaffeensis* to subvert innate host defense for infection and survival is essential for understanding intracellular pathogen infection strategies and provides a model to investigate molecular host-pathogen interactions involved in repurposing host signaling pathways for infection.

RESULTS

***E. chaffeensis* TRP120 shared sequence homology and predicted Notch ligand function.** We previously showed TRP120 interacts with Notch activating metalloprotease, ADAM17, and Notch antagonist FBW7 using yeast-two hybrid analysis (Y2H) (8). We also showed that TRP120 binds to the promoter region of *notch1* using chromatin immunoprecipitation sequencing (ChIP-Seq), and that activation of Notch occurred during infection (6, 10). Notch activation occurs through direct interaction of Notch ligands with the Notch-1 receptor initiating two receptor proteolytic cleavages, resulting in NICD nuclear translocation and subsequent activation of Notch downstream targets. Because TRP120 has been shown to activate the Notch signaling pathway, we examined TRP120 sequence homology and correlates of biological functionality with Notch ligands.

NCBI protein basic local alignment search tool (BLAST) was used to identify local similarity between TRP120 and canonical/noncanonical Notch ligand sequences. Sequence homology with a TRP120 tandem repeat (TR) IDD motif, TESHQKEDEIVSQPSSE (aa 284 to 301), was shown to share sequence homology with several canonical Notch ligands, including Jagged-1, DLL1, DLL4, and noncanonical Notch ligand TSP2 (Fig. 1A). We then used the informational spectrum method (ISM) to predict similar functional properties between TRP120 and Notch ligands. ISM is a prediction method that uses the electron-ion interaction potential of each amino acid within the primary sequence of proteins to translate the primary sequences into numerical sequences. Translated sequences were then converted into a spectrum using a Fourier transform. Cross spectral analysis of the translated sequences was performed to obtain characteristic frequency peaks that demonstrated if proteins share a similar biological function. TRP120 was predicted to share a similar biological function with canonical Notch ligands, DLL 1, 3, and 4, and noncanonical Notch ligand F3 contactin-1, a known adhesion molecule (Fig. S1A to D). To identify the sequence responsible for the identified frequency peaks, reverse Fourier transform of ISM was performed (Fig. 1B). A 35-mer TRP120-TR IDD motif, IVSQPSSEPFVAESEVSKVEQ EETNPEVLIKDLQD (aa 214 to 248 and 294 to 328), was associated with characteristic frequency peaks (Fig. 1B and C). Collectively, these results indicated that the TRP120 sequence and fundamental biophysical properties of the amino acids were consistent with Notch ligands.

A.

```
TRP120    284-TESHQKEDEIVSQPSSE-301
               :*:  :**::  ::  ::
Jagged-1  1160-HNSEVEEDDMDKHQQKA-1172

TRP120    284-TESHQKEDEIVSQPSSE-301
              .:.*:*:*   .**:::
DLL1      655-RDAHSKRDTK-CQPQGS-671

TRP120    284-TESHQKEDEIVSQPSSE-301
              .:::::* *:  .*:*:::
DLL4      397-SNCEKKVDRCTSNPCAN-413

TRP120    284-TESHQKEDEIVSQPSSE-301
              **  :  *:*    :*:
TSP2      970-VIRHQGK-ELVQTANSD-999
```

B.
214 – <u>IVSQPSSE</u>PFVAESEVSKVEQEETNPEVLIKDLQD – 248

C.

TESHQKEDE<u>IVSQPSSE</u>
▭ BLAST Sequence Homology/<u>ISM</u>

FIG 1 *E. chaffeensis* TRP120 shares sequence homology and biological function with canonical and noncanonical Notch ligands. (A) BLAST analysis of TRP120 with canonical/noncanonical Notch ligands demonstrating amino acid homology. An asterisk (*) represents identical conserved amino acid residues; a colon (:) represents conservative substitutions. (B) The informational spectrum method (ISM) was used to predict if TRP120 shared a similar biological function with canonical and noncanonical Notch ligands. Primary sequences of TRP120 and Notch ligands were converted into a numerical sequence-based electron-ion interaction potential (EIIP) of each amino acid. Numerical sequences were converted into a spectrum using Fourier transform. To determine if proteins shared a similar biological function cross spectra analysis was performed and similar biological function is denoted by a peak at a frequency of F(0.288). (C) Schematic of TRP120 N- C- (gray) and TR domains (blue) with four highlighted repetitive TRP120 TR motifs that share sequence homology with Notch ligands. ISM sequence is shown in (B) (underlined). (*) represents a partial tandem repeat-containing similar (EDDTVSQPSLE) but nonidentical sequence to highlighted sequence.

***E. chaffeensis* TRP120 directly interacted with the Notch-1 ligand-binding region (LBR).** Canonical activation of the Notch pathway is known to occur through canonical Notch ligands binding to Notch receptor LBD (EGFs 11 to 13 in the extracellular domain [ECD]). To investigate if TRP120 interacts with the Notch-1 receptor LBR (EGFs 1 to 15), we ectopically expressed GFP-tagged full-length TRP120 (TRP120-FL-GFP) in HeLa cells and probed for endogenous Notch-1 to determine colocalization. Pearson's correlation coefficient (PC) and Mander's coefficient (MC) (correlation range +1 to −1; 0 represented absence of correlation) were used to quantify the degree of colocalization between TRP120-FL-GFP and Notch-1. Ectopically expressed TRP120-FL-GFP was found to strongly colocalize (PC = 0.897 and MC = 0.953) with endogenous Notch-1 (Fig. 2A). In comparison, ectopically expressed AcGFP-vector showed no colocalization (PC = 0.008 and MC = 0.009) with endogenous Notch-1 (Fig. 2A). Colocalization of TRP120 and Notch-1 demonstrates that these two proteins are in the same spatial location. However, it does not demonstrate direct protein-protein interaction. To confirm a direct interaction, we utilized pulldown assays of recombinant TRP120-FL (rTRP120-FL) and rNotch-1 LBR, and a direct protein-protein interaction was demonstrated (Fig. 2B and Fig. S2A and B). Recombinant thioredoxin (rTRX) was the fusion tag for the pBAD expression vector used to express the rTRP120 constructs. Therefore, rTRX was used as a negative recombinant control, and no interaction was observed (Fig. 2B). Based on sequence homology and ISM data, a short region of sequence homology within the tandem repeat (TR) domain was identified that could be involved in the TRP120 and Notch-1 LBR. To determine if the TRP120-TR was responsible for the previous TRP120 and Notch-1 LBR interaction, we performed a pulldown assay with rTRP120-TR and rNotch-1 LBR. rTRP120-TR was pulled down with Fc-tagged rNotch-1 LBR, demonstrating a direct interaction with the TR domain (Fig. 2C).

To further confirm the direct interaction of rTRP120-FL or rTRP120-TR and rNotch-1 LBR, surface plasmon resonance (SPR) was performed. Interaction between both
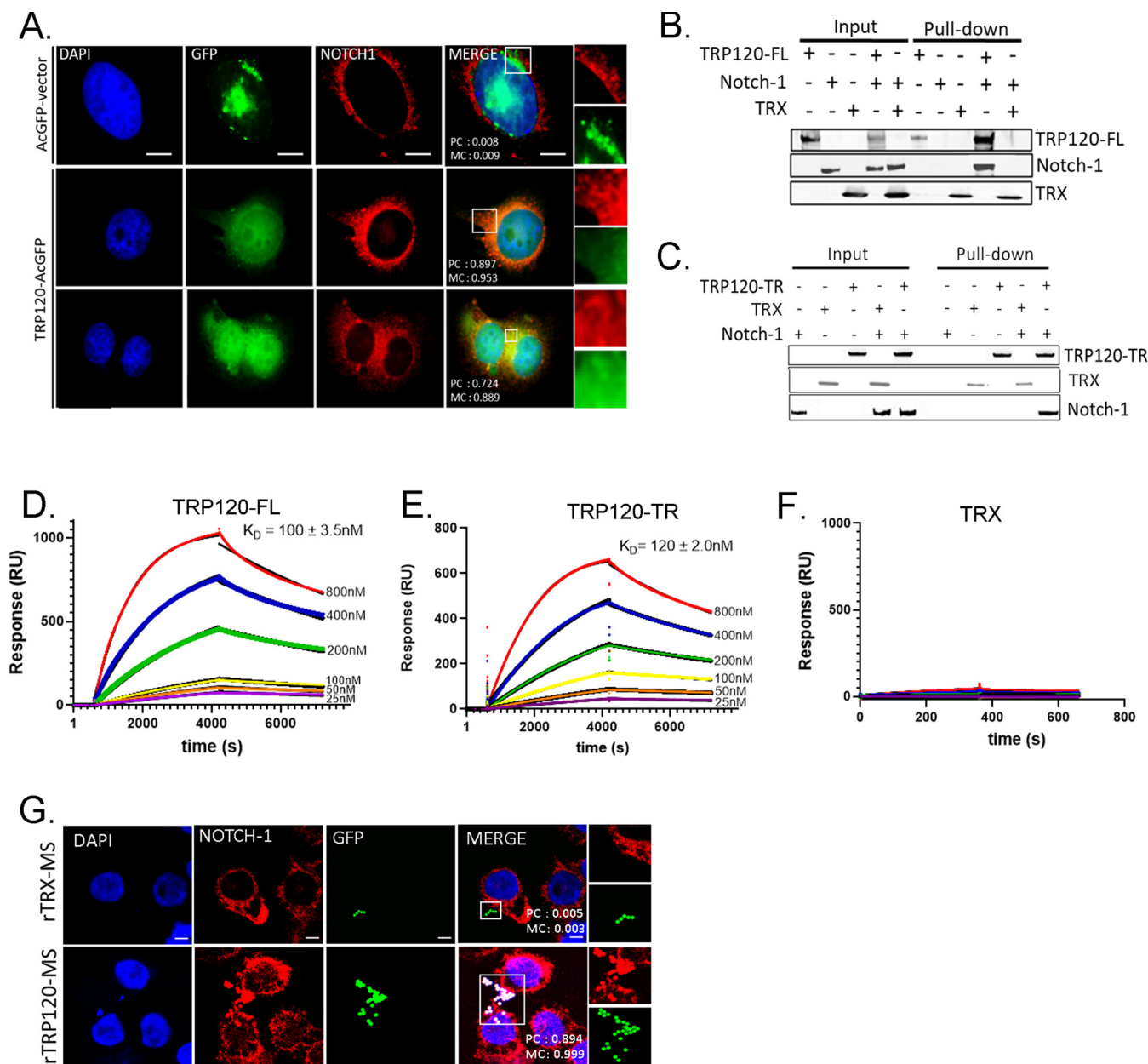
FIG 2 *E. chaffeensis* TRP120-TR interactions with the Notch receptor ligand-binding region (LBR). (A) HeLa cells transfected with TRP120-GFP (green) and probed for endogenous Notch-1 (red) demonstrated colocalization by immunofluorescent microscopy. Colocalization was quantitated by Pearson's and Mander's coefficients (0 no colocalization; +1 strong colocalization). (B and C) His tag pulldown assays demonstrated a direct interaction between TRP120 and Notch-1. rFc-tagged Notch-1 LBR was incubated with (B) TRP120-FL-His, (C) TRP120-TR-His, or TRX-His negative-control on Talon metal affinity resin. Bound Notch-1, TRP120-His, α-TRP120 against a TR peptide or TRX-His were detected with α-Notch-1, α-TRP120, or α-TRX antibodies. (D-F) Surface plasmon resonance of (D) TRP120-FL-His, (E) TRP120-TR-His, or (F) TRX-His with Fc-tagged Notch-1 LBR on a Biacore T100 with a series S Ni-nitrilotriacetic acid (NTA) sensor chip. TRP120-FL-His, TRP120-TR-His, or TRX-His were immobilized on the NTA chip and 2-fold dilutions (800 nM to 25 nM) of Fc-tagged Notch-1 LBR were used as an analyte to determine binding affinity (K_D). Sensograms and K_D are representative of data from triplicate experiments. (G) THP-1 cells were treated with rTRX- or rTRP120-FL-coated fluorescent microspheres for 1h. Colocalization was visualized by confocal immunofluorescent microscopy. Notch-1 was immunostained with tetramethylrhodamine isothiocyanate (TRITC) and TRP120-coated fluorescein isothiocyanate (FITC) auto-fluorescent microspheres. Nuclei were stained with DAPI (blue). White boxes indicate areas of colocalization measurements. Scale bar = 10 μm. (H) Dot blot of PBS, TRX, or TRP120-FL-coated microspheres probed with α-TRX or α-TRP120 antibodies, respectively.

rTRP120-FL (Fig. 2D) and rTRP120-TR (Fig. 2E) with rNotch-1 LBR was detected in a concentration-dependent manner. Fitting the concentration-response plots for rTRP120-FL and rTRP120-TR yielded a K_D (equilibrium dissociation constant) of 100 ± 3.5 nM and 120 ± 2.0 nM, respectively (Fig. 2D and E). No interaction was detected between rTRX and rNotch-1 LBR (Fig. 2F). Additionally, treatment of THP-1 cells with rTRP120-coated sulfate, yellow-green microspheres demonstrated colocalization of rTRP120 and Notch-
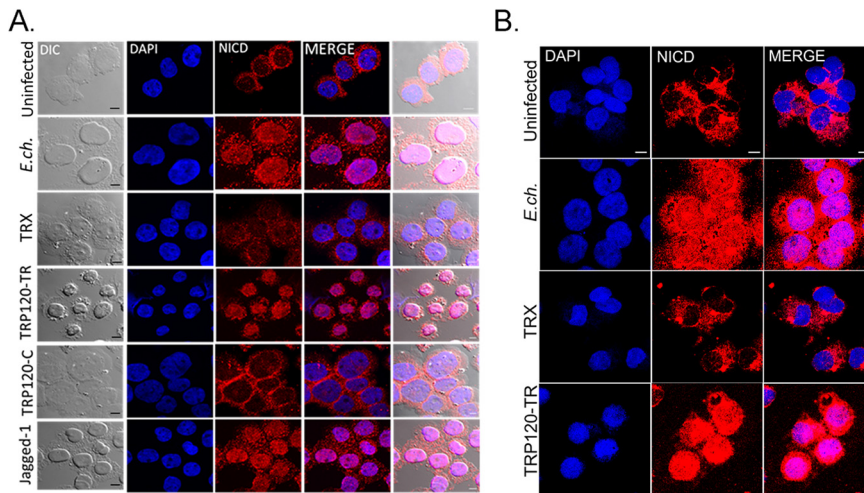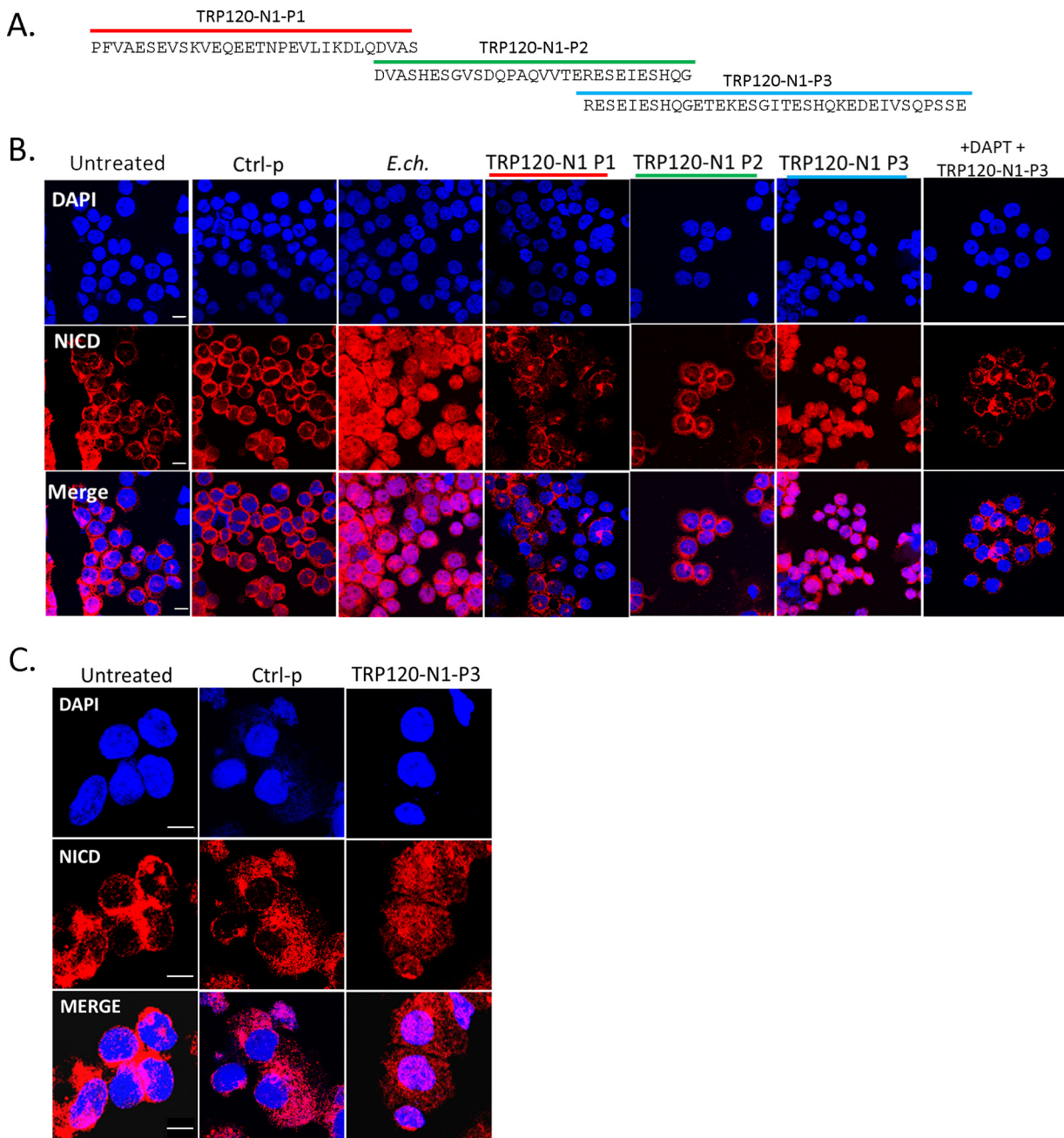
FIG 3 TRP120-TR activates Notch and NICD nuclear translocation in primary human monocytes. (A) Soluble recombinant TRP120-TR or -C-terminal proteins (2 μg/mL) were incubated with THP-1 cells for 2 h. Cells were collected and NICD localization was determined by confocal immunofluorescent microscopy. Uninfected/untreated or recombinant TRX-treated THP-1 cells were used as negative controls. *E. chaffeensis*-infected or recombinant Jagged-1 treated THP-1 cells were used as positive controls. NICD nuclear translocation was detected in *E. chaffeensis*-infected, TRP120-TR and Jagged-1 treated cells. (B) Primary human monocytes were treated with soluble TRP120-TR or recombinant TRX as described above and NICD nuclear translocation was detected in *E. chaffeensis*-infected and TRP120-TR-treated cells. Endpoint analysis was performed as described in Fig. 2. Experiments were performed in triplicate and representative images are shown.

1 (Fig. 2G). In comparison, the rTRX-coated fluorescent microsphere did not colocalize with the Notch-1 receptor (Fig. 2G). rTRP120 and rTRX coating of sulfate, yellow-green microspheres were confirmed using dot blot (Fig. S3) Together, these binding data revealed rTRP120-TR bound the rNotch-1 LBR.
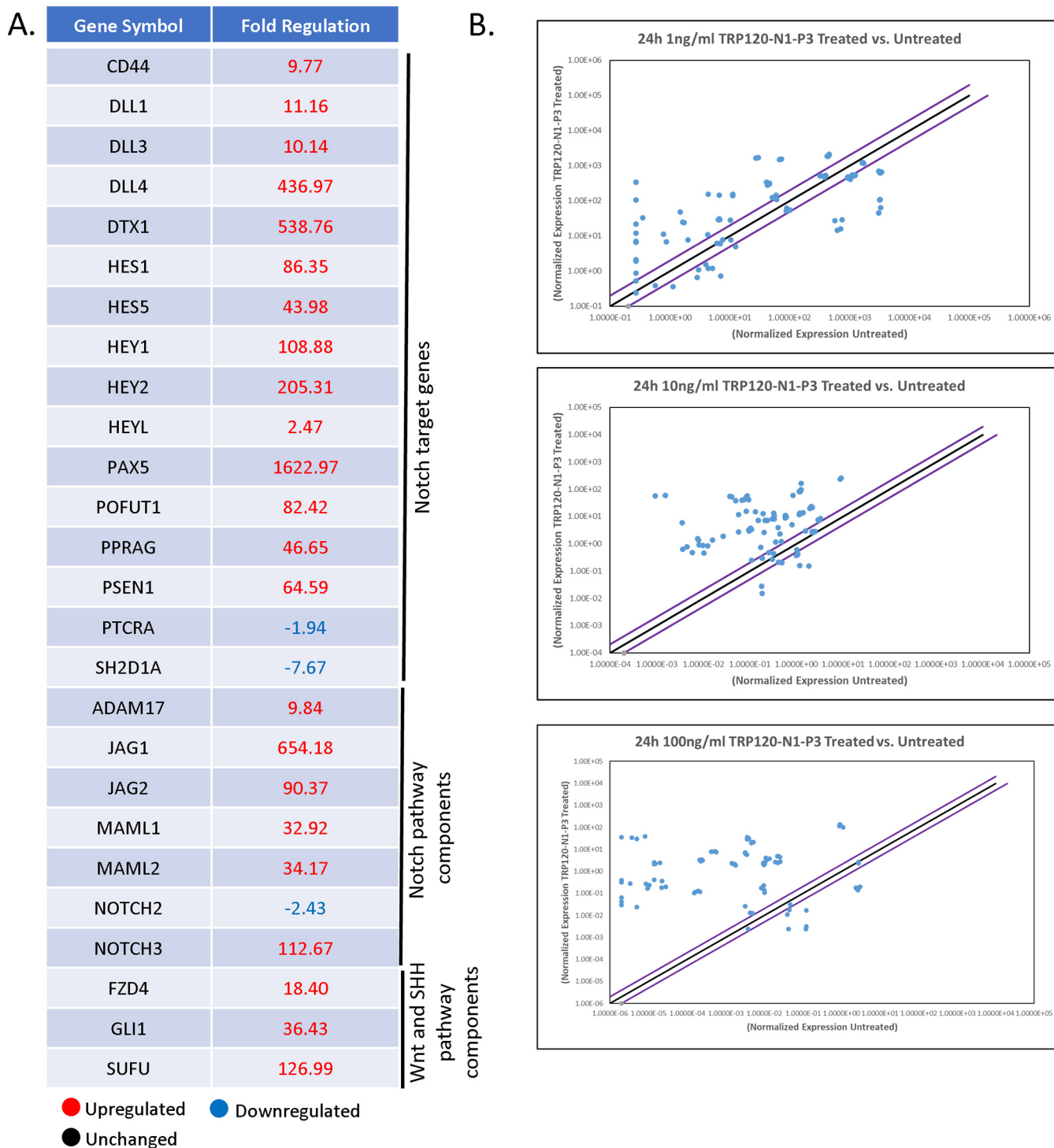
E. chaffeensis TRP120-TR domain was required for Notch activation. Both the N-terminal MNNL and cysteine-rich DSL domain of Notch ligands are known to be required for receptor binding. However, there is little known regarding ligand motifs required for Notch activation. We previously demonstrated Notch activation occurred in THP-1 cells after stimulation with TRP120-coated beads for 15 min (6). Gene expression levels of *notch1*, *hes1*, and *hes5* were upregulated after incubation with TRP120-coated beads. To further delineate the TRP120 domain required for Notch activation, THP-1 cells or primary human monocytes were treated with soluble purified truncated constructs of rTRP120 (rTRP120-TR and rTRP120-C terminus) (Fig. S2A-B). THP-1 cells infected with *E. chaffeensis* or treated with rJagged-1 were used as positive controls and demonstrated NICD nuclear translocation 2 h posttreatment (pt). In comparison, rTRP120-TR caused NICD nuclear translocation 2 h posttreatment (Fig. 3A and B). NICD nuclear translocation was not observed in untreated cells, cells treated with TRX or rTRP120-C-terminal soluble proteins (Fig. 3A and B). Collectively, these data demonstrated the requirement of TRP120-TR for Notch activation.

E. chaffeensis TRP120-TR Notch ligand IDD-mimetic activated Notch. To determine if Notch is activated by a TRP120-TR Notch mimetic IDD motif, several TRP120-TR synthetic peptides were generated (Fig. 4A). THP-1 cells or primary human monocytes were treated with TRP120-TR IDD peptides for 2 h. THP-1 cells infected with *E. chaffeensis* were used as a positive-control and scrambled peptide was used as the negative-control. A 35-aa TRP120-TR IDD motif (TRP120-N1-P3) caused NICD nuclear translocation (Fig. 4B and C) compared with scrambled negative-control treated cells. Importantly, the TRP120-TR IDD contained a motif identified in both sequence homology and ISM data (Fig. 1C). Inhibition of Notch signaling by DAPT, a γ-secretase inhibitor, abrogated Notch activation with TRP120-N1-P3 treatment, indicating that TRP120-N1-P3 directly binds to the Notch-1 receptor for Notch activation (Fig. 4B). To confirm Notch activation by TRP120-N1-P3, gene expression levels of Notch downstream targets were examined by human Notch

A.

TRP120-N1-P1

PFVAESEVSKVEQEETNPEVLIKDLQDVAS

TRP120-N1-P2

DVASHESGVSDQPAQVVTERESEIESHQG

TRP120-N1-P3

RESEIESHQGETEKESGITESHQKEDEIVSQPSSE

B.

C.

FIG 4 A TRP120-TR Notch-1 memetic IDD peptide stimulates NICD nuclear translocation. (A) Overlapping TRP120-TR IDD peptide sequences (P1-P3) (B) THP-1 cells or (C) Primary human monocytes were incubated with synthetic TRP120-TR IDD peptides to determine the TRP120-TR Notch-1 memetic motif responsible for Notch activation. TRP120-TR peptides were overlapping peptides spanning an entire TR domain. Cells were treated with peptide (1 μg/mL) for 2 h and confocal immunofluorescent microscopy was used to visualize NICD localization. NICD nuclear translocation denotes Notch activation. A scrambled peptide (Ctrl-p) was used as negative control and *E. chaffeensis*-infected cells were used as positive control. To determine if direct interaction of the TRP120-N1-P3 peptide and Notch receptor was necessary for Notch activation, THP-1 cells were pretreated with DAPT, a γ-secretase inhibitor, and treated with TRP120-N1-P3 peptide for 2 h.

signaling pathway array analysis. In comparison with untreated THP-1 cells, a significant increase in Notch downstream targets, including HES1, HES5, HEY1, and HEY2 gene expression levels occurred in TRP120-N1-P3 treated cells (Fig. 5A and B, Table S1A). Interestingly, Notch gene expression by TRP120-N1-P3 treatment was increased in a concentration-dependent manner (Fig. 5B, Table S1A). Importantly, rJagged-1 also demonstrated similar upregulation of Notch genes in a concentration-dependent manner (Fig. S4). These data demonstrated that a TRP120 IDD mimetic motif was responsible for TRP120 Notch activation.

A.

Gene Symbol	Fold Regulation	
CD44	9.77	Notch target genes
DLL1	11.16	
DLL3	10.14	
DLL4	436.97	
DTX1	538.76	
HES1	86.35	
HES5	43.98	
HEY1	108.88	
HEY2	205.31	
HEYL	2.47	
PAX5	1622.97	
POFUT1	82.42	
PPRAG	46.65	
PSEN1	64.59	
PTCRA	-1.94	
SH2D1A	-7.67	
ADAM17	9.84	Notch pathway components
JAG1	654.18	
JAG2	90.37	
MAML1	32.92	
MAML2	34.17	
NOTCH2	-2.43	
NOTCH3	112.67	
FZD4	18.40	Wnt and SHH pathway components
GLI1	36.43	
SUFU	126.99	

🔴 Upregulated 🔵 Downregulated
⚫ Unchanged

B.

FIG 5 TRP120-N1-P3 IDD peptide stimulates Notch gene expression. (A) Table of Notch pathway genes with corresponding fold change displaying differential expression (up, down or no change) at 24 h pt with 10 ng/mL of TRP120-N1-P3 peptide (B) Scatterplots of expression array analysis of 84 Notch signaling pathway genes to determine Notch gene expression 24 h after stimulation with 1 ng/mL (top), 10 ng/mL (middle) or 100 ng/mL (bottom) of TRP120-N1-P3 peptide. Purple lines denote a 2-fold upregulation or downregulation in comparison to control, and the black line denotes no change. Scatterplots are representative of three independent experiments (*n* = 3).
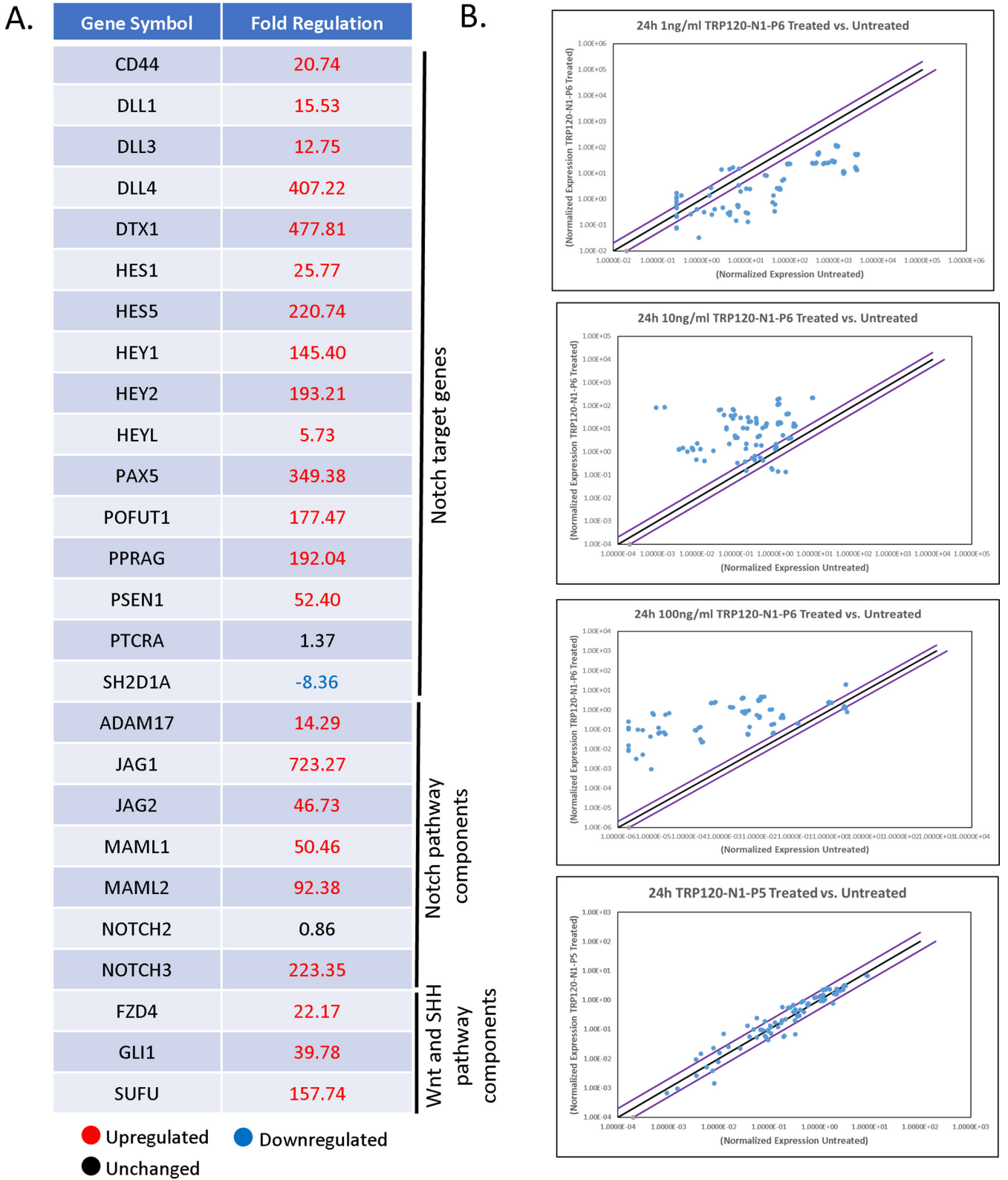
***E. chaffeensis* TRP120-TR Notch ligand SLiM mimetic activates Notch.** It is well-documented that SLiMs are found in two general groups: posttranslational modification (PTM) motifs and ligand motifs that mediate binding events. We previously identified a functional TRP120 HECT E3 ligase catalytic motif located in the C terminus (2, 7) and have
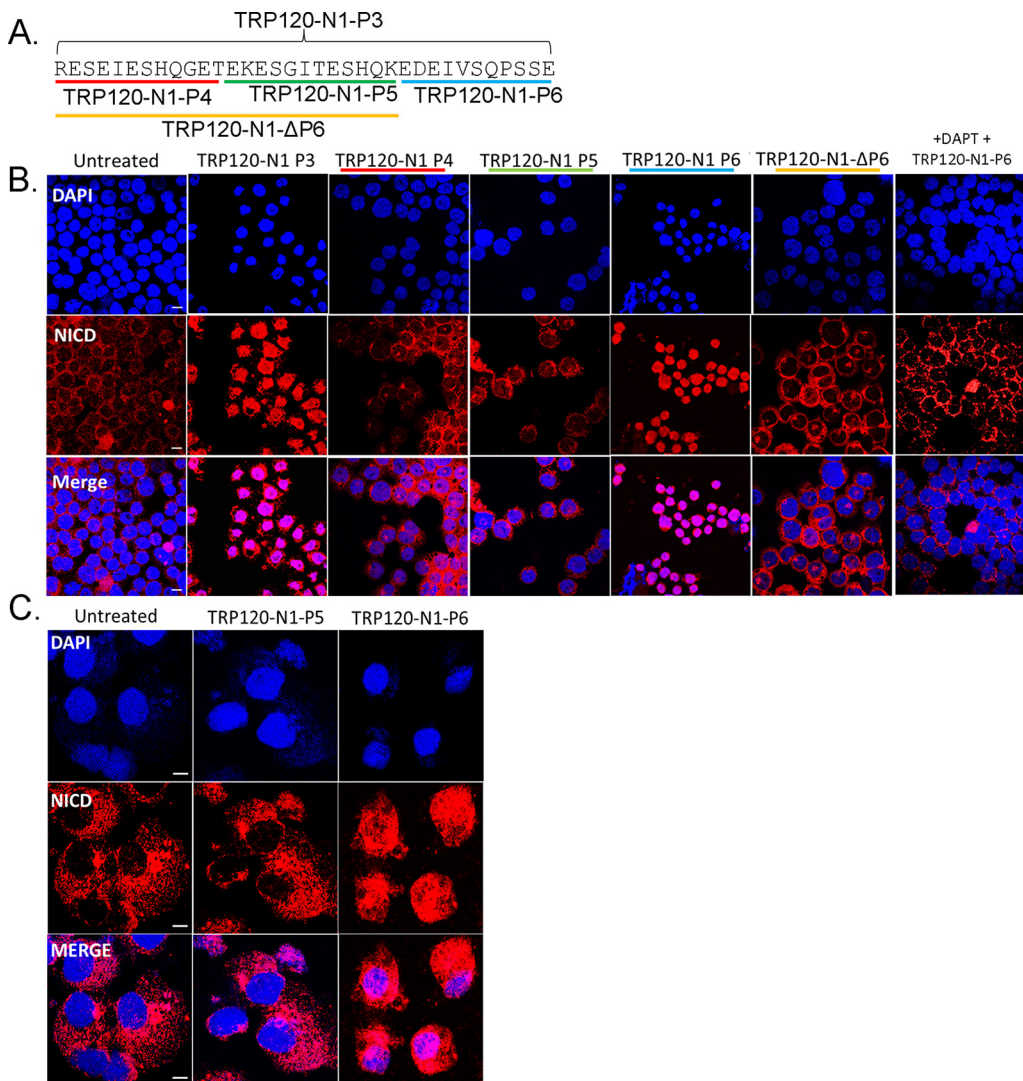
FIG 6 A TRP120-TR Notch-1 memetic SLiM peptide activates Notch signaling. (A) TRP120-N1 SLiM (P4-P6) and TRP120-N1-ΔP6 peptide sequences. (B) THP-1 cells or (C) primary human monocytes were treated with synthetic TRP120-TR SLiM peptides to identify the TRP120-TR Notch-1 SLiM memetic motif. TRP120-TR peptides were SLiM peptides spanning the entire TRP120-N1-P3 peptide sequence. TRP120-N1-P6 deletion mutant peptide has a deletion of the TRP120-N1-P6 amino acids. Cells were treated with peptide (1 μg/mL) for 2 h and NICD localization visualized by confocal microscopy. TRP120-N1-P3 peptide was used as a positive control. To determine if direct interaction of the TRP120-N1-P6 peptide and Notch receptor was necessary for Notch activation, THP-1 cells were pretreated with DAPT, a γ-secretase inhibitor, and treated with TRP120-N1-P6 peptide for 2 h. Representative data of all experiments are shown (n = 3).

recently identified a TRP120-TR Wnt SLiM mimetic motif (3). To determine if the TRP120-TR Notch mimetic motif could be a SLiM (aa 3 to 12), overlapping TRP120-TR synthetic peptides that span the identified 35-aa TRP120-TR IDD motif were synthesized (Fig. 6A). Treatment with P4 or P5 TRP120-TR Notch mimetic SLiM peptides in THP-1 cells did not result in NICD nuclear translocation (Fig. 6B). However, TRP120-TR Notch mimetic SLiM P6 (TRP120-N1-P6) located at the C terminus resulted in NICD nuclear translocation (Fig. 6B). TRP120-N1-P6 was also shown to cause NICD nuclear translocation in primary human monocytes (Fig. 6C). Furthermore, pretreatment of DAPT inhibited TRP120-N1-P6 Notch activation (Fig. 6B). Upregulation of Notch downstream targets occurred with TRP120-N1-P6 treatment in a concentration-dependent manner (Fig. 7A and B, Table S1B), as previously shown with the TRP120-N1-P3 peptide. In comparison, TRP120-N1-P5 peptide treatment did not result in significant upregulation of Notch gene expression (Fig. 7B).

A.

Gene Symbol	Fold Regulation
CD44	20.74
DLL1	15.53
DLL3	12.75
DLL4	407.22
DTX1	477.81
HES1	25.77
HES5	220.74
HEY1	145.40
HEY2	193.21
HEYL	5.73
PAX5	349.38
POFUT1	177.47
PPRAG	192.04
PSEN1	52.40
PTCRA	1.37
SH2D1A	-8.36
ADAM17	14.29
JAG1	723.27
JAG2	46.73
MAML1	50.46
MAML2	92.38
NOTCH2	0.86
NOTCH3	223.35
FZD4	22.17
GLI1	39.78
SUFU	157.74

Notch target genes (CD44 through SH2D1A)
Notch pathway components (ADAM17 through NOTCH3)
Wnt and SHH pathway components (FZD4 through SUFU)

🔴 Upregulated   🔵 Downregulated   ⚫ Unchanged

B.

FIG 7 TRP120-N1-P6 SLiM Notch memetic peptide stimulates Notch gene expression. (A) Selected Notch pathway genes with corresponding fold change displaying differential expression (upregulation and downregulation) at 24 h pt with 10 ng/mL of TRP120-N1-P6 peptide. (B) Scatterplots of expression array analysis of 84 Notch signaling pathway genes to determine Notch gene expression with 1 ng/mL, 10 ng/mL, 100 ng/mL of TRP120-N1-P6 peptide or TRP120-N1-P5 treatment (10 ng/mL) compared to untreated cells (bottom) at 24 pt. Purple lines denote a 2-fold upregulation or downregulation in comparison to control, and the black lines denote no change. Scatterplots are representative of three independent experiments (*n* = 3).
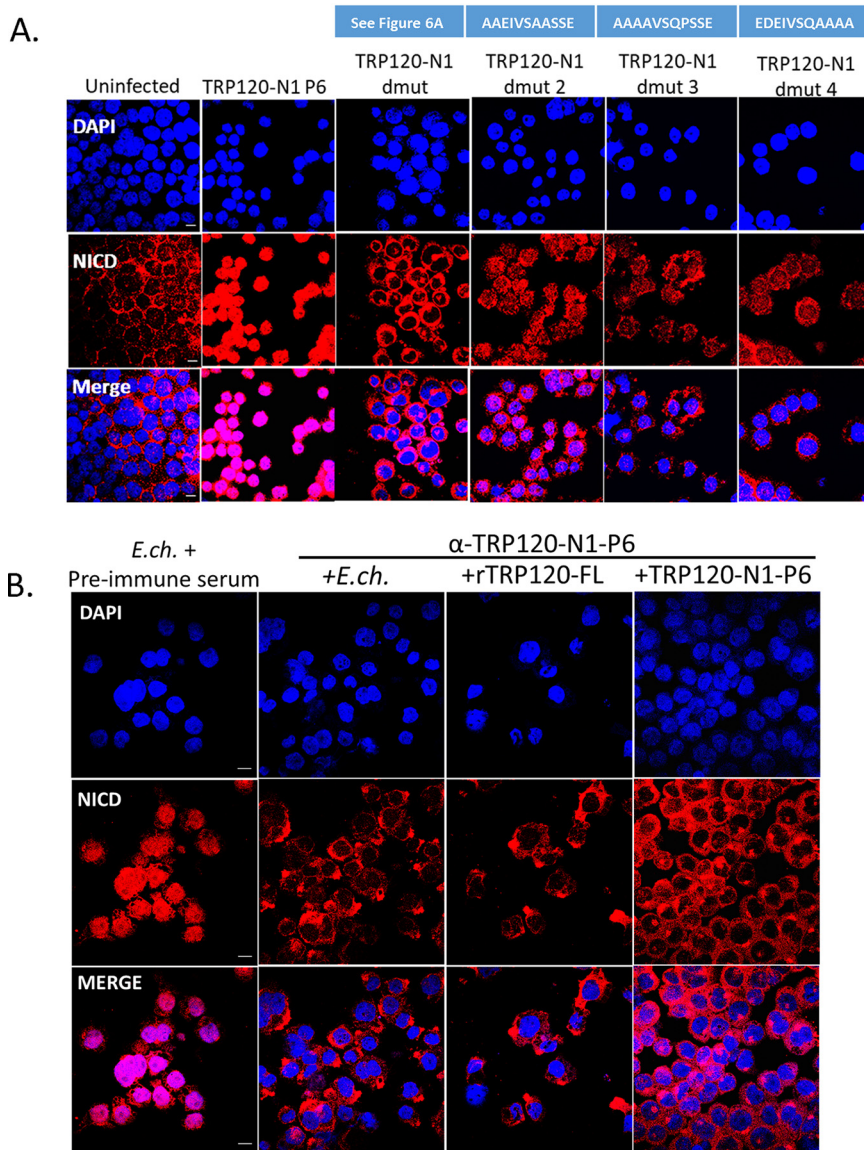
FIG 8 Amino acids critical to TRP120-N1-P6 memetic SLiM activity and anti-SLiM antibody blocks Notch activation (A) Critical amino acids of the TRP120-N1-P6 memetic SLiM determined by alanine mutagenesis (mutant peptide sequences are shown above the corresponding panel). THP-1 cells were treated with mutant peptides (dmut2, -3, and -4; 1 μg/mL) for 2 h and confocal immunofluorescent microscopy was used to visualize NICD localization. NICD nuclear translocation denotes Notch activation. Peptide TRP120-N1-ΔP6 peptide was used as a negative-control and TRP120-N1-P6 was used as a positive control. (B) Cell-free *E. chaffeensis*, rTRP120-FL, or TRP120-N1-P6 were incubated with α-TRP120-N1-P6 rabbit polyclonal antibody (5 μg/mL) for 30 min. Preimmune serum was used as a control antibody. THP-1 cells were subsequently inoculated with the cell-free *E. chaffeensis*/ α-TRP120-N1-P6 mixture for 2 h and confocal immunofluorescent microscopy was used to visualize NICD nuclear localization. Representative data of all experiments are shown ($n = 3$).

To confirm that TRP120-N1-P6 is required for Notch activation, a TRP120-N1-P6 deletion mutant peptide (TRP120-N1-ΔP6) (Fig. 6A) was tested. THP-1 cells stimulated with TRP120-N1-ΔP6 peptide exhibited abrogated Notch activation as demonstrated by NICD translocation (Fig. 6B). To determine the residues required in the TRP120-TR Notch mimetic SLiM, alanine mutagenesis of mutant peptides dmut-2, -3, and -4 was performed to determine the contribution of specific amino acids to Notch activation (Fig. 8A, blue boxes). Mutated residues were selected based on sequence homology and ISM data. Mutants (TRP120-N1-ΔP6, dmut-2, -3, and -4) exhibited reduced Notch activation as determined by NICD translocation, but only the TRP120-N1-ΔP6 peptide

resulted in full abrogation of NICD nuclear translocation (Fig. 8A). Collectively, these data demonstrated that the TRP120-N1-P6 SLiM was a Notch mimetic.

TRP120 Notch SLiM antibody blocked *E. chaffeensis* Notch activation. To investigate whether the TRP120 Notch mimetic is solely responsible for Notch activation by *E. chaffeensis*, THP-1 cells were pretreated with a purified rabbit polyclonal antibody generated against the TRP120-N1-P6 SLiM and subsequently infected with *E. chaffeensis* for 2 h. Negative preimmune serum was used as a negative control. NICD nuclear translocation was determined in α-TRP120-N1-P6 SLiM or negative preimmune serum treated cells. THP-1 cells treated with α-TRP120-N1-P6 SLiM did not display NICD nuclear translocation, in comparison to the negative preimmune serum control (Fig. 8B). These data suggested that TRP120-N1-P6 SLiM was the only Notch mimic involved in Notch activation by *E. chaffeensis*.

DISCUSSION

We previously demonstrated TRP120-host interactions to occur with a diverse array of host cell proteins associated with conserved signaling pathways, including Wnt and Notch (8). Two proteins shown to interact with TRP120 were the Notch metalloprotease, a disintegrin and metalloprotease domain (ADAM17), and a Notch antagonist, F-box and WD repeat domain-containing 7 (FBW7). In addition, we demonstrated that *E. chaffeensis* and rTRP120 activate Notch signaling to downregulate TLR2/4 expression for intracellular survival. However, the molecular mechanisms utilized for TRP120 Notch activation have not been previously studied (6). Moreover, Keewan et al. (31), demonstrated activation of Notch signaling during *Mycobacterium avium paratuberculosis* (MAP) infection. Notch-1 signaling was shown to modulate macrophage polarization and immune defenses during infection, but the molecular mechanisms were not defined (31). In this study, we investigated the molecular interactions involved in TRP120 Notch activation and defined a TRP120 Notch SLiM mimetic responsible for Notch activation.

Molecular mimicry has been well-established as an evolutionary survival strategy utilized by pathogens to disrupt or coopt host function as a protective mechanism to avoid elimination by the host immune system (30, 32–36). More specifically, SLiMs are a distinct, intrinsically disordered class of protein interaction motifs that have been shown to evolve *de novo* for promiscuous binding to various partners and have been documented as a host hijacking mechanism for pathogens (26, 29, 30). Although SLiM mimicry has been established as a mechanism utilized by pathogens to repurpose host cell functions for survival, a Notch ligand mimic has never been defined.

TRP120 is a type 1 secretion system (T1SS) effector that is found on the surface of infectious dense-cored *E. chaffeensis* and is also secreted into the host cell after entry, where it translocates to the host cell nucleus. TRP120 contains four intrinsically disordered tandem repeat (TR) domains that have been previously described as important for TRP120's moonlighting capabilities (9, 12). Within these intrinsically disordered domains are various SLiMs responsible for TRP120 multifunctionality. We recently defined a novel TRP120 repetitive SLiM that activates Wnt signaling to promote *E. chaffeensis* infection (3). In the current study, we also determined TRP120-TR as the domain responsible for Notch activation. Sequence homology studies and information spectrum method (ISM) have shown sequence similarity and similar biological function between TRP120 and endogenous Notch ligands. ISM is a virtual spectroscopy method utilized to predict if proteins share a similar biological function based on the electron-ion interaction potential of amino acids, and only requires the nucleotide sequence of each protein. It was recently used to determine the prediction of the potential receptor, natural reservoir, tropism, and therapeutic/vaccine target of severe acute respiratory syndrome coronavirus 2 (SARS-CoV-2) (37). Our results demonstrated a shared sequence similarity and biological function with both canonical and noncanonical Notch ligands that occurred within the tandem repeat domain of TRP120 (TRP120-TR). Both sequence homology and ISM studies identified specific tandem repeat sequences that are functionally associated with endogenous Notch ligands and range between 20 and 35 amino acids in size. These data suggested that intrinsically

disordered regions found within the TRP120-TR domain are responsible for Notch ligand mimic function and direct effector-host protein interaction with the Notch receptor.

Notch ligand binding occurs specifically with EGFs 11 to 13 within the LBR of the Notch receptor (37, 38). Canonical Notch ligands are known to contain a DSL domain that is important for Notch binding and activation, but a conserved activation motif has not been defined. Colocalization of TRP120 with Notch-1 was previously shown to occur during *E. chaffeensis* infection (6). However, a direct interaction was not previously shown using yeast-two hybrid (8), possibly due to limitations of this technique with protein interactions involving membrane proteins (6, 39). Using pull-down, SPR, and protein-coated fluorescent microsphere approaches, we further studied TRP120-Notch-1 interaction and found direct binding occurs through TRP120-TR at a Notch-1 LBR (EGFs 1 to 15). TRP120-TR and Notch-1 LBR interaction occurred at an affinity of 120 $\pm$ 2.0 nM, indicating a strong protein-protein interaction. Numerous structural studies of interactions of Notch with endogenous ligands have shown low-affinity interactions between Notch Jag or DLL ECDs (40–42). One study demonstrated weak affinities between Notch-1 with an engineered high-affinity Jag-1 variant (K_D = 5.4 μM) and DLL4 (12.8 μM) (37). The higher binding affinity of TRP120-TR in comparison to canonical Notch ligands suggests that the four tandemly repeated motifs folds in a structure that potentiates binding between TRP120 and Notch-1. In addition, stimulating THP-1 cells and primary monocytes with TRP120-TR resulted in NICD nuclear translocation, indicating that TRP120-TR is the TRP120 domain responsible for Notch activation. Interestingly, TRP120-Fzd5 interaction also occurred through the tandem repeat domain and supports our current findings that TRP120-host protein interactions occur within regions of the tandem repeat domain, likely due to its disordered nature (3).

Secreted and membrane-bound proteins have been shown to activate Notch signaling. These noncanonical Notch ligands lack the DSL domain but still can modify Notch signaling. Some of the noncanonical Notch proteins contain EGF-like domains. However, others share very little sequence similarity to endogenous Notch ligands (23, 43). TSP2 is a secreted mammalian protein containing EGF-like domains. TSP2 was found to potentiate Notch signaling by direct Notch-3/Jagged1 binding (44). Furthermore, TSP2 binds directly to purified Notch-3 protein containing EGF-like domains 1 to 11, suggesting a direct interaction. Non-canonical Notch ligand TSP2 was found to share significant sequence homology within the TRP120-TR sequence. Homologous regions included the identified TRP120-TR Notch SLiM mimetic. Although TSP2 has been identified as a secreted, noncanonical Notch ligand, there has been no activating motif identified to date. F3/contactin1, another identified secreted noncanonical Notch ligand, does not contain DSL or EGF-like domains. However, it activates the Notch signaling pathway through the Notch-1 receptor (45). TRP120 was found to share biological function with F3/contactin1 by ISM. F3/contactin1 has been demonstrated to bind to Notch-1 at two different locations within the NECD and activates Notch signaling when presented as a purified soluble protein (45). Therefore, Notch activation by secreted, noncanonical Notch ligands has been demonstrated. However, more insight into the molecular details of those interactions needs to be elucidated. TRP120 is found on the surface of infectious dense-cored *Ehrlichia* (46) and contributes to the internalization of *E. chaffeensis* by activation of the Wnt pathway (4). Thus, during infection, TRP120 likely activates Notch signaling as a surface-bound protein when *E. chaffeensis* encounters the host cell as was demonstrated with the whole *E. chaffeensis* (Fig. 9). In addition, we also demonstrated that soluble TRP120 and peptides can activate Notch signaling. This is a significant finding that could have implications with regard to the systemic effects of TRP120 that may be released during infection. Moreover, these findings provide new information regarding the activation of Notch signaling by soluble ligands, which were previously thought to require cell to cell interaction. This study provides new insight regarding noncanonical Notch ligand activation of the Notch signaling pathway.

SLiMs have been identified in secreted effector proteins of intracellular bacterial pathogens, including *Ehrlichia*, *Anaplasma phagocytophilum* (47), *Legionella pneumophila* (48–50), and *Mycobacterium tuberculosis* (51). This investigation identifies a novel
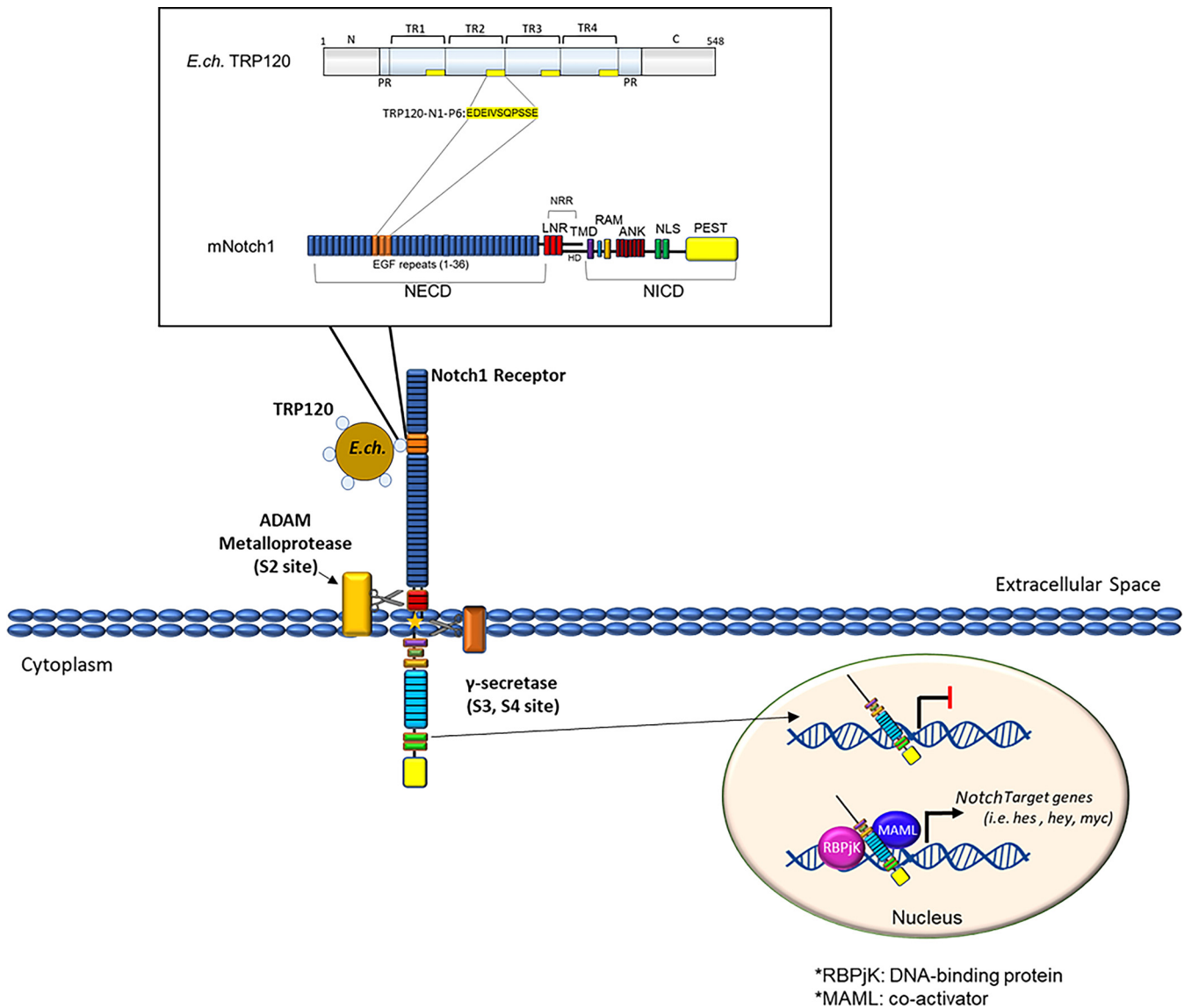
FIG 9 Proposed model of *E. chaffeensis* TRP120 Notch activation. A TRP120-TR Notch SLiM memetic motif (TRP120-N1-P6; yellow highlight) binds the Notch-1 extracellular domain at a region containing the confirmed Notch ligand-binding domain (LBD) to activate Notch signaling. TRP120-N1-P6 binding leads to NICD nuclear translocation and upregulation of Notch gene targets.

Notch SLiM (11 aa) that can activate Notch signaling as a soluble ligand. Complete NICD nuclear translocation was previously shown to occur at 2 h postinfection (6), indicating that NICD nuclear translocation during *E. chaffeensis* infection is a result of TRP120-TR Notch ligand SLiM mimetic interaction with the Notch-1 receptor. In addition, Notch signaling pathway genes were upregulated at 24 h in TRP120-TR Notch mimetic SLiM-treated THP-1 cells. These data are consistent with our previous findings where we detected upregulation of Notch signaling pathway components and target genes during *E. chaffeensis* infection at 12, 24, 48, and 72 h pi, with maximum changes in Notch gene expression occurring at 24 h pi (6). Furthermore, during *E. chaffeensis* infection, TRP120 mediated ubiquitination, and proteasomal degradation of Notch negative regulator, FBW7 begins at 24 h pi and gradually decreases during late stages of infection (2). Both TRP120 and FBW7 are localized to the nucleus beginning at 24 h pi, suggesting that TRP120 degradation of FBW7 assists in upregulation of Notch downstream targets at this time point (2).

Interestingly, both the TRP120 Notch memetic IDD (TRP120-N1-P3) and SLiM (TRP120-N1-P6) resulted in concentration-dependent upregulation of Notch downstream targets

(Fig. 5B and Fig. 7B). Similar to our findings, studies have shown that the Notch pathway can induce heterogeneous phenotypic responses in a Notch ligand or NICD dose-dependent manner. Klein et al. (52) demonstrated that high levels of Notch ligands can induce a ligand inhibitory effect, while lower levels of Notch ligand activate Notch signaling activity. Similarly, Semenova et al. (53) showed that NICD and Jag1 transduction increases osteogenic differentiation in a dose-dependent manner. However high dosage of NICD and Jag1 decreases osteogenic differentiation efficiency. Furthermore, Gomez-Lamarca et al. (54) showed that NICD dosage can influence CSL-DNA binding kinetics, NICD dimerization, and chromatin opening to strengthen transcriptional activation. Therefore, an increase in Notch ligand-receptor interaction may lead to increased NICD release and Notch signaling strength.

Alanine mutagenesis demonstrated the entire 11-aa TRP120-TR Notch ligand SLiM mimetic is required for Notch activation. Importantly, SLiMs are known to have low-affinity, transient protein-protein interactions within the low-micromolar range (26). In this case, the repeated TRP120-TR Notch ligand SLiM mimetic motif may cause TRP120 to fold in a tertiary structure upon binding to the Notch-1 receptor that stabilizes the TRP120-Notch-1 interaction. Based on these data, *E. chaffeensis* TRP120 could be used as a model to study SLiMs within intrinsically disordered effector proteins that are utilized for host exploitation by other intracellular bacterial pathogens.

To demonstrate that TRP120-TR Notch ligand SLiM mimetic motif is solely responsible for *E. chaffeensis* activation of Notch, we generated an antibody against the mimetic epitope to block *E. chaffeensis is* TRP120-Notch-1 binding. Our results demonstrated antibody blockade of Notch activation by *E. chaffeensis*, rTRP120, and the TRP120-TR Notch ligand SLiM peptide. These data strongly support the conclusion that the TRP120-TR Notch ligand SLiM mimetic is responsible for *E. chaffeensis* Notch activation and may provide a new *E. chaffeensis* therapeutic target. Hence, this study serves to provide insight into the molecular details of how Notch signaling is modulated during *E. chaffeensis* infection and may serve as a model for other pathogens.

Further outstanding questions regarding the regulation of the Notch signaling pathway during *E. chaffeensis* remain. We recently demonstrated maintenance of Notch activation is linked to TRP120-mediated ubiquitination and proteasomal degradation of tumor suppressor FBW7, a Notch negative regulator (2). However, other potential Notch regulators may serve as a target for TRP120-mediated ubiquitination for constitutive Notch activation during infection. Suppressor of Deltex (Su[dx]) is an E3 ubiquitin ligase that serves as another negative regulator of Notch signaling by degrading Deltex, a positive regulator of Notch signaling (55). Su(dx) may serve as another target of TRP120-mediated ubiquitination to maintain Notch activity during *E. chaffeensis* infection. Furthermore, how secreted noncanonical Notch ligands can cause separation between the NICD and NECD remains unknown. TRP120 causes Notch activation, resulting in upregulation of Notch downstream targets. However, the mechanism of how the S2 exposure for ADAM cleavage is not understood. Future crystallography studies on TRP120 and Notch-1 interaction may provide more insight into these structural details required for TRP120-N1-P6 SLiM Notch activation (56, 57).

In conclusion, we demonstrated *E. chaffeensis* Notch activation is initiated by a TRP120 Notch SLiM mimetic. Our findings have identified a pathogen protein host mimic to repurpose the evolutionarily conserved Notch signaling pathway for intracellular survival. This study gives more insight into how obligate intracellular pathogens, with small genomes, have evolved host mimicry modules *de novo* to exploit conserved signaling pathways to suppress innate defenses to promote infection.

MATERIALS AND METHODS

Cell culture and cultivation of *E. chaffeensis*. Human monocytic leukemia cells (THP-1; ATCC TIB-202) were propagated in RPMI medium (ATCC) containing 2 mM L-glutamine, 10 mM HEPES, 1 mM sodium pyruvate, 4500 mg/liter glucose, 1500 mg/liter sodium bicarbonate, supplemented with 10% fetal bovine serum (fetal bovine serum [FBS]; Invitrogen) at 37°C in 5% CO_2 atmosphere. *E. chaffeensis* (Arkansas strain) was cultivated in THP-1 cells. Host cell-free *E. chaffeensis* was prepared by rupturing infected THP-1 cells or primary human monocytes with sterile glass beads (1 mm) by vortexing. Infected

THP-1 cells were harvested and pelleted by centrifugation at 500 × *g* for 5 min. The pellet was resuspended in sterile phosphate-buffered saline (PBS) in a 50 mL tube containing glass beads and vortexed at moderate speed for 1 min. The cell debris was pelleted at 1,500 × *g* for 10 min, and the supernatant was further pelleted by high-speed centrifugation at 12,000 × *g* for 10 min, 4°C. The purified *Ehrlichia* were resuspended in a fresh RPMI medium and utilized as needed.

Human peripheral blood mononuclear cell (PBMC) and primary monocyte isolation. Primary human monocytes were isolated from 125 mL of human blood obtained from the Gulf Coast Regional Blood Center (Houston, TX). Blood was diluted in RMPI medium and separated by density gradient separation on Ficoll at 2000 rpm for 20 min. The plasma was removed from the separated sample and the buffy coat was collected. Buffy coat was diluted with DPBS containing 2% FBS and 1 mM EDTA and centrifuged at 1500 rpm for 15 min. The supernatant was removed, and all cells were combined and mixed carefully. Combined cells were then centrifuged at 1500 rpm for 10 min, and the supernatant was removed. Cells were resuspended into 1 mL of Dulbecco's PBS (DPBS) containing 2% FBS and 1 mM EDTA. Cells were then diluted to 5×10^7 cells/mL, and monocytes were separated by the EasySep Human Monocyte Enrichment kit without CD16 depletion (Stemcell number 19058) according to the manufacturer's protocol. Primary human monocytes were then cultured in RPMI medium (ATCC) containing 2 mM L-glutamine, 10 mM HEPES, 1 mM sodium pyruvate, 4500 mg/liter glucose,1500 mg/liter sodium bicarbonate, supplemented with 10% fetal bovine serum (FBS; Invitrogen) at 37°C in 5% CO_2 atmosphere.

Antibodies and reagents. Primary antibodies used in this study for immunofluorescence microscopy, Western blot analysis, and pulldown assays include monoclonal rabbit α-Notch1 (3608S; Cell Signaling Technology, Danvers MA), polyclonal rabbit α-Notch1, intracellular (07-1231; Millipore Sigma, Billerica, MA), rabbit α-TRP120-I1 (58) polyclonal rabbit α-TRX (T0803; Sigma-Aldrich, Saint Louis, MO). Polyclonal rabbit anti-TRP120 antiserum was commercially generated against a TRP120 epitope inclusive of aa 290 to 301 (GenScript, Piscataway, NJ). Synthetic peptides used in this study were commercially generated (Genscript, Piscataway, NJ).

Sequence homology. Genome and transcriptome sequences encoding *E. chaffeensis* TRP120 and *Homo sapiens* Notch ligand proteins were recovered using BLAST searches with the online version at the NCBI website. Sequences were submitted to NCBI Protein BLAST and ClustalW2 sequence databases for sequence alignment.

Informational spectrum method (ISM). ISM analyzes the primary structure of proteins by assigning a physical parameter that is relevant for the protein's biological function (59, 60). Each amino acid in TRP120 and Notch ligand sequences was given a value corresponding to its electron-ion interaction potential (EIIP), which determines the long-range properties of biological molecules. The value of the amino acids within the protein was Fourier transformed to provide a Fourier spectrum that is representative of the protein, resulting in a series of frequencies and amplitudes. The frequencies correspond to a physicochemical property involved in the biological activity of the protein. Comparison of proteins is performed by cross-spectra analysis. Proteins with similar spectra were predicted to have a similar biological function. Inverse Fourier Transform was performed to identify the sequence responsible for obtained signals at a given frequency.

Transfection. HeLa cells (1×10^6) were seeded in a 60 mm culture dish 24 h before transfection. AcGFP-TRP120 or AcGFP-control plasmids were added to Opti-MEM and Lipofectamine 2000 mixture and incubated for 20 min at 37°C. Lipofectamine/plasmid mixtures were added to HeLa cells and incubated for 4 h at 37°C. The medium was aspirated 4 h posttransfection and fresh medium was added to each plate and incubated for 24 h.

Pull-down assay. Recombinant His tagged TRP120 (10 μg) and Notch-1 (10 μg) (Sino Biological) were incubated with Ni-NTA beads alone or in combination for 4 h at 4°C. Supernatants were collected and the Ni-NTA beads were washed 5× with 10 mM imidazole wash buffer. Proteins were eluted off with 200 mM imidazole elution buffer and binding were determined by Western blotting.

Immunofluorescent confocal microscopy. THP-1 cells (2×10^6) were treated with full-length or truncated constructs (-TR or -C terminus) of recombinant TRP120 or TRP120 peptides for 2 h at 37°C. Cells were collected and fixed using 4% formaldehyde, washed with 1× PBS, and permeabilized and blocked in 0.5% Triton X-100 and 2% bovine serum albumin (BSA) in PBS for 30 min. Cells were washed with PBS and probed with polyclonal rabbit α-Notch-1, intracellular (1:100) (Millipore Sigma, MA) or monoclonal rabbit α-Notch1 (3608S; Cell Signaling Technology, Danvers MA) for 1 h at room temperature. Cells were washed with PBS and probed with Alexa Fluor 568 rabbit anti-goat IgG (H+L) for 30 min at room temperature, washed, and then mounted with ProLong Gold antifade reagent with DAPI (Molecular Probes, OR). Slides were imaged on a Zeiss LSM 880 confocal laser scanning microscopy. Pearson's correlation coefficient and Mander's correlation coefficient were generated by ImageJ software to quantify the degree of colocalization between fluorophores.

Protein-coated fluorescent microsphere assay. TRP120 and TRX recombinant proteins were desalted using Zeba spin desalting columns (Thermo Fisher Scientific, MA) as indicated by the manufacturer protocol. The protein abundance of desalted recombinant protein was assessed by bicinchoninic acid assay (BCA assay). One-micrometer, yellow-green (505/515), sulfate FluoSpheres (Life Technologies, CA) were first equilibrated with 40 μM MES buffer followed by incubation with 10 μg of desalted TRP120 or TRX recombinant protein in 40 μM MES (2-[N-morpholino] ethanesulfonic acid) buffer for 2 h at room temperature on a rotor. TRP120 or TRX coated FluoSpheres were washed twice with 40 μM MES buffer at 12,000 × *g* for 5 min and then resuspended in RPMI medium. To determine the TRP120 or TRX protein coating of FluoSpheres, dot blotting of FluoSpheres samples was performed after protein coating using α-TRX or α-TRP120 antibodies. 8×10^5 THP-1 cells/well were plated in a 96-well round-bottom

plate, and the TRP120 or TRX coated FluoSpheres were added to each well at approximately 5 beads/cell. The cell and protein-coated FluoSpheres were incubated between 5 and 60 min at 37°C with 5% CO^2, collected and unbound beads were washed twice with $1\times$ PBS, followed by fixation by cytospin for 15 min. Cell samples were then processed for analysis by immunofluorescent confocal microscopy, as previously mentioned. FluoSpheres are light-sensitive, therefore all steps were performed in the dark.

Quantitative real-time PCR. The human Notch signaling targets PCR array profiles the expression of 84 Notch pathway-focused genes to analyze Notch pathway status. PCR arrays were performed according to the PCR array handbook from the manufacturer. Briefly, uninfected and *E. chaffeensis*-infected or Notch mimetic peptide-treated THP-1 cells were collected at 24 and 48 h intervals, and RNA purification with minor modifications, cDNA synthesis, and real-time PCR were performed as previously described (3).

Western blot analysis. Cells were lysed in RIPA lysis buffer (0.5 M Tris-HCl, pH 7.4, 1.5 M NaCl, 2.5% deoxycholic acid, 10% NP-40, 10 mM EDTA) containing protease inhibitor cocktail for 30 min at 4°C. Lysates were then cleared by centrifugation and protein abundance was assessed by bicinchoninic acid assay (BCA assay). Samples were added to Laemelli buffer then boiled for 5 min. Lysates were then subjected to SDS-PAGE followed by transfer to nitrocellulose membrane. Membranes were blocked for 1 h in 5% nonfat milk diluted in TBST and then exposed to α-TRP120, α-TRX, or α-Notch-1 primary antibodies overnight. Membranes were washed three times in Tris-buffered saline containing 1% Triton (TBST) for 30 min followed by 1 h of incubation with horseradish peroxidase-conjugated anti-rabbit and anti-mouse secondary antibodies (SeraCare, Milford, MA) (diluted 1:10,000 in 5% nonfat milk in TBST). Proteins were visualized with ECL via Chemi-doc2 and densitometry was measured with VisionWorks image acquisition and analysis software.

Surface plasmon resonance. SPR was performed using a BIAcore T100 instrument with nitrilotriacetic acid (NTA) sensor chip. Purified polyhistidine-tagged, full-length, rTRP120-TR, rTRX and human rNotch-1 Fc Chimera Protein, CF (R&D Systems, MN) were dialyzed in running buffer (100 mM sodium phosphate [pH 7.4], 400 mM NaCl, 40 μM EDTA, 0.005% [vol/vol]). Briefly, each cycle of running started with charging the NTA chip with 500 μM $NiCl^2$. Subsequently, purified polyhistidine-tagged, full-length, truncated rTRP120 proteins, or rTRX (0.1 μM) were immobilized on the NTA sensor as the ligand on flow cell 2. Immobilization was carried out at 25°C at a constant flow rate of 30 μL/min for 100s. Various concentrations of Notch1-NECD constructs (0 to 800 nM) were injected over sensor surfaces as analytes with duplicates along with several blanks of running buffer. Injections of analyte were carried out at a flow rate of 30 μL/min with a contact time of 360 s and a dissociation time of 300 s. Finally, the NTA surface was regenerated by using 350 mM EDTA. Readout included a sensorgram plot of response against time, showing the progress of the interaction. Curve fittings were done with the 1:1 Langmuir binding model with all fitting quality critique requirements met. The binding affinity (K_D) was determined for all interactions by extracting the association rate constant and dissociation rate constant from the sensorgram curve (K_D = Kd/Ka) using the BIAevaluation package software.

TRP120 antibody inhibition of *E. chaffeensis* Notch activation. Host cell-free *E. chaffeensis* was pretreated with 5 to 10 μg/mL of polyclonal rabbit anti-TRP120 antibody generated against the TRP120 Notch mimetic SLiM (aa 284 to 301), or purified IgG antibody. The cell-free *E. chaffeensis*/antibody mixture was then added to THP-1 cells (5×10^5) in a 12-well plate for 2 h. Samples were collected, washed with PBS, and prepared for Immunofluorescent microscopy.

TRP120 protein expression and purification. Full length or truncated constructs of rTRP120, or rTRX control were expressed in a pBAD expression vector, which has been previously optimized by our laboratory (58, 61, 62). Recombinant TRP120 full-length, truncated constructs, and rTRX were purified via nickel-nitrilotriacetic acid (Ni-NTA) purification system. All recombinant proteins were dialyzed via PBS and tested for bacterial endotoxins using the Limulus amebocyte lysate (LAL) test.

Statistical analysis. All data are represented as the means $\pm$ standard deviation (SD) of data obtained from at least three independent experiments done with triplicate biological replicates unless otherwise indicated. Analyses were performed using a two-way ANOVA or two-tailed Student's *t* test (GraphPad Prism 6 software, La Jolla, CA). $P < 0.05$ was considered statistically significant.

SUPPLEMENTAL MATERIAL

Supplemental material is available online only.

FIG S1, TIF file, 0.5 MB.
FIG S2, TIF file, 0.5 MB.
FIG S3, TIF file, 0.02 MB.
FIG S4, TIF file, 0.6 MB.
TABLE S1, XLSX file, 0.01 MB

REFERENCES

1. Jaworski DC, Cheng C, Nair ADS, Ganta RR. 2017. Amblyomma americanum ticks infected with in vitro cultured wild-type and mutants of Ehrlichia chaffeensis are competent to produce infection in naive deer and dogs. Ticks Tick Borne Dis 8:60–64. https://doi.org/10.1016/j.ttbdis.2016.09.017.

2. Wang JY, Zhu B, Patterson LL, Rogan MR, Kibler CE, McBride JW. 2020. *Ehrlichia chaffeensis* TRP120-mediated ubiquitination and proteasomal degradation of tumor suppressor FBW7 increases oncoprotein stability and promotes infection. PLoS Pathog 16:e1008541. https://doi.org/10.1371/journal.ppat.1008541.

3. Rogan MR, Patterson LL, Byerly CD, Luo T, Paessler S, Veljkovic V, Quade B, McBride JW. 2021. Ehrlichia chaffeensis TRP120 is a Wnt ligand mimetic that interacts with Wnt Receptors and contains a novel repetitive short linear motif that activates Wnt signaling. mSphere 6:e00216-21. https://doi.org/10.1128/mSphere.00216-21.

4. Luo T, Dunphy PS, Lina TT, McBride JW. 2015. *Ehrlichia chaffeensis* exploits canonical and noncanonical host Wnt signaling pathways to stimulate phagocytosis and promote intracellular survival. Infect Immun 84:686–700. https://doi.org/10.1128/IAI.01289-15.

5. Lina TT, Luo T, Velayutham TS, Das S, McBride JW. 2017. *Ehrlichia* activation of Wnt-PI3K-mTOR signaling inhibits autolysosome generation and autophagic destruction by the mononuclear phagocyte. Infect Immun 85. https://doi.org/10.1128/IAI.00690-17.

6. Lina TT, Dunphy PS, Luo T, McBride JW. 2016. Ehrlichia chaffeensis TRP120 activates canonical notch signaling to downregulate TLR2/4 expression and promote intracellular survival. mBio 7:e00672-16. https://doi.org/10.1128/mBio.00672-16.

7. Zhu B, Das S, Mitra S, Farris TR, McBride JW. 2017. *Ehrlichia chaffeensis* TRP120 moonlights as a HECT E3 ligase involved in self and host ubiquitination to influence protein interactions and stability for intracellular survival. Infect Immun 85. https://doi.org/10.1128/IAI.00290-17.

8. Luo T, Kuriakose JA, Zhu B, Wakeel A, McBride JW. 2011. *Ehrlichia chaffeensis* TRP120 interacts with a diverse array of eukaryotic proteins involved in transcription, signaling, and cytoskeleton organization. Infect Immun 79:4382–4391. https://doi.org/10.1128/IAI.05608-11.

9. Klema VJ, Sepuru KM, Fullbrunn N, Farris TR, Dunphy PS, McBride JW, Rajarathnam K, Choi KH. 2018. *Ehrlichia chaffeensis* TRP120 nucleomodulin binds DNA with disordered tandem repeat domain. PLoS One 13:e0194891. https://doi.org/10.1371/journal.pone.0194891.

10. Zhu B, Kuriakose JA, Luo T, Ballesteros E, Gupta S, Fofanov Y, McBride JW. 2011. *Ehrlichia chaffeensis* TRP120 binds a G+C-rich motif in host cell DNA and exhibits eukaryotic transcriptional activator function. Infect Immun 79:4370–4381. https://doi.org/10.1128/IAI.05422-11.

11. Mitra S, Dunphy PS, Das S, Zhu B, Luo T, McBride JW. 2018. *Ehrlichia chaffeensis* TRP120 effector targets and recruits host polycomb group proteins for degradation to promote intracellular infection. Infect Immun 86:e00845-17. https://doi.org/10.1128/IAI.00845-17.

12. Byerly CD, Patterson LL, McBride JW. 2021. Ehrlichia TRP effectors: moonlighting, mimicry and infection. Pathog Dis 79:ftab026. https://doi.org/10.1093/femspd/ftab026.

13. Baonza A, Garcia-Bellido A. 2000. Notch signaling directly controls cell proliferation in the Drosophila wing disc. Proc Natl Acad Sci U S A 97:2609–2614. https://doi.org/10.1073/pnas.040576497.

14. Urbanek K, Lesiak M, Krakowian D, Koryciak-Komarska H, Likus W, Czekaj P, Kusz D, Sieroń AL. 2017. Notch signaling pathway and gene expression profiles during early in vitro differentiation of liver-derived mesenchymal stromal cells to osteoblasts. Lab Invest 97:1225–1234. https://doi.org/10.1038/labinvest.2017.60.

15. Zweidler-McKay PA, He Y, Xu L, Rodriguez CG, Karnell FG, Carpenter AC, Aster JC, Allman D, Pear WS. 2005. Notch signaling is a potent inducer of growth arrest and apoptosis in a wide range of B-cell malignancies. Blood 106:3898–3906. https://doi.org/10.1182/blood-2005-01-0355.

16. Artavanis-Tsakonas S, Rand MD, Lake RJ. 1999. Notch signaling: cell fate control and signal integration in development. Science 284:770–776. https://doi.org/10.1126/science.284.5415.770.

17. Nakano N, Nishiyama C, Yagita H, Koyanagi A, Ogawa H, Okumura K. 2011. Notch1-mediated signaling induces MHC class II expression through activation of class II transactivator promoter III in mast cells. J Biol Chem 286:12042–12048. https://doi.org/10.1074/jbc.M110.138966.

18. Hoyne GF. 2003. Notch signaling in the immune system. J Leukoc Biol 74:971–981. https://doi.org/10.1189/jlb.0303089.

19. Sarin A, Marcel N. 2017. The NOTCH1-autophagy interaction: regulating self-eating for survival. Autophagy 13:446–447. https://doi.org/10.1080/15548627.2016.1268303.

20. Palaga T, Ratanabunyong S, Pattarakankul T, Sangphech N, Wongchana W, Hadae Y, Kueanjinda P. 2013. Notch signaling regulates expression of Mcl-1 and apoptosis in PPD-treated macrophages. Cell Mol Immunol 10:444–452. https://doi.org/10.1038/cmi.2013.22.

21. Miele L, Osborne B. 1999. Arbiter of differentiation and death: Notch signaling meets apoptosis. J Cell Phys 181:393–409. https://doi.org/10.1002/(SICI)1097-4652(199912)181:3%3C393::AID-JCP3%3E3.0.CO;2-6.

22. Chillakuri CR, Sheppard D, Lea SM, Handford PA. 2012. Notch receptor-ligand binding and activation: insights from molecular studies. Semin Cell Dev Biol 23:421–428. https://doi.org/10.1016/j.semcdb.2012.01.009.

23. D'Souza B, Miyamoto A, Weinmaster G. 2008. The many facets of Notch ligands. Oncogene 27:5148–5167. https://doi.org/10.1038/onc.2008.229.

24. Edwards RJ, Davey NE, O'Brien K, Shields DC. 2012. Interactome-wide prediction of short, disordered protein interaction motifs in humans. Mol Biosyst 8:282–295. https://doi.org/10.1039/c1mb05212h.

25. Kumar M, Gouw M, Michael S, Sámano-Sánchez H, Pancsa R, Glavina J, Diakogianni A, Valverde JA, Bukirova D, Čalyševa J, Palopoli N, Davey NE, Chemes LB, Gibson TJ. 2020. ELM-the eukaryotic linear motif resource in 2020. Nucleic Acids Res 48:D296–D306. https://doi.org/10.1093/nar/gkz1030.

26. Van Roey K, Uyar B, Weatheritt RJ, Dinkel H, Seiler M, Budd A, Gibson TJ, Davey NE. 2014. Short linear motifs: ubiquitous and functionally diverse protein interaction modules directing cell regulation. Chem Rev 114:6733–6778. https://doi.org/10.1021/cr400585q.

27. Davey NE, Van Roey K, Weatheritt RJ, Toedt G, Uyar B, Altenberg B, Budd A, Diella F, Dinkel H, Gibson TJ. 2012. Attributes of short linear motifs. Mol Biosyst 8:268–281. https://doi.org/10.1039/c1mb05231d.

28. Dunphy PS, Luo T, McBride JW. 2014. *Ehrlichia chaffeensis* exploits host SUMOylation pathways to mediate effector-host interactions and promote intracellular survival. Infect Immun 82:4154–4168. https://doi.org/10.1128/IAI.01984-14.

29. Davey NE, Trave G, Gibson TJ. 2011. How viruses hijack cell regulation. Trends Biochem Sci 36:159–169. https://doi.org/10.1016/j.tibs.2010.10.002.

30. Via A, Uyar B, Brun C, Zanzoni A. 2015. How pathogens use linear motifs to perturb host cell networks. Trends Biochem Sci 40:36–48. https://doi.org/10.1016/j.tibs.2014.11.001.

31. Keewan E, Naser SA. 2020. Notch-1 Signaling Modulates Macrophage Polarization and Immune Defense against Mycobacterium avium paratuberculosis Infection in Inflammatory Diseases. Microorganisms 8:1006. https://doi.org/10.3390/microorganisms8071006.

32. Drayman N, Glick Y, Ben-Nun-Shaul O, Zer H, Zlotnick A, Gerber D, Schueler-Furman O, Oppenheim A. 2013. Pathogens use structural mimicry of native host ligands as a mechanism for host receptor engagement. Cell Host Microbe 14:63–73. https://doi.org/10.1016/j.chom.2013.05.005.

33. Mondino S, Schmidt S, Buchrieser C. 2020. Molecular mimicry: a paradigm of host-microbe coevolution illustrated by legionella. mBio 11:e01201-20. https://doi.org/10.1128/mBio.01201-20.

34. Price CT, Al-Khodor S, Al-Quadan T, Santic M, Habyarimana F, Kalia A, Kwaik YA. 2009. Molecular mimicry by an F-box effector of Legionella pneumophila hijacks a conserved polyubiquitination machinery within macrophages and protozoa. PLoS Pathog 5:e1000704. https://doi.org/10.1371/journal.ppat.1000704.

35. Chemes LB, de Prat-Gay G, Sanchez IE. 2015. Convergent evolution and mimicry of protein linear motifs in host-pathogen interactions. Curr Opin Struct Biol 32:91–101. https://doi.org/10.1016/j.sbi.2015.03.004.

36. Dunphy PS, Luo T, McBride JW. 2013. *Ehrlichia* moonlighting effectors and interkingdom interactions with the mononuclear phagocyte. Microbes Infect 15:1005–1016. https://doi.org/10.1016/j.micinf.2013.09.011.

37. Luca VC, Kim BC, Ge C, Kakuda S, Wu D, Roein-Peikar M, Haltiwanger RS, Zhu C, Ha T, Garcia KC. 2017. Notch-Jagged complex structure implicates a catch bond in tuning ligand sensitivity. Science 355:1320–1324. https://doi.org/10.1126/science.aaf9739.

38. Whiteman P, de Madrid BH, Taylor P, Li D, Heslop R, Viticheep N, Tan JZ, Shimizu H, Callaghan J, Masiero M, Li JL, Banham AH, Harris AL, Lea SM, Redfield C, Baron M, Handford PA. 2013. Molecular basis for Jagged-1/Serrate ligand recognition by the Notch receptor. J Biol Chem 288: 7305–7312. https://doi.org/10.1074/jbc.M112.428854.

39. Bruckner A, Polge C, Lentze N, Auerbach D, Schlattner U. 2009. Yeast two-hybrid, a powerful tool for systems biology. Int J Mol Sci 10:2763–2788. https://doi.org/10.3390/ijms10062763.

40. Andrawes MB, Xu X, Liu H, Ficarro SB, Marto JA, Aster JC, Blacklow SC. 2013. Intrinsic selectivity of Notch 1 for Delta-like 4 over Delta-like 1. J Biol Chem 288:25477–25489. https://doi.org/10.1074/jbc.M113.454850.

41. Kershaw NJ, Church NL, Griffin MD, Luo CS, Adams TE, Burgess AW. 2015. Notch ligand delta-like1: X-ray crystal structure and binding affinity. Biochem J 468:159–166. https://doi.org/10.1042/BJ20150010.

42. Cordle J, Johnson S, Tay JZ, Roversi P, Wilkin MB, de Madrid BH, Shimizu H, Jensen S, Whiteman P, Jin B, Redfield C, Baron M, Lea SM, Handford PA. 2008. A conserved face of the Jagged/Serrate DSL domain is involved in Notch trans-activation and cis-inhibition. Nat Struct Mol Biol 15:849–857. https://doi.org/10.1038/nsmb.1457.

43. Wang MM. 2011. Notch signaling and Notch signaling modifiers. Int J Biochem Cell Biol 43:1550–1562. https://doi.org/10.1016/j.biocel.2011.08.005.

44. Meng H, Zhang X, Hankenson KD, Wang MM. 2009. Thrombospondin 2 potentiates notch3/jagged1 signaling. J Biol Chem 284:7866–7874. https://doi.org/10.1074/jbc.M803650200.

45. Hu QD, Ang BT, Karsak M, Hu WP, Cui XY, Duka T, Takeda Y, Chia W, Sankar N, Ng YK, Ling EA, Maciag T, Small D, Trifonova R, Kopan R, Okano H, Nakafuku M, Chiba S, Hirai H, Aster JC, Schachner M, Pallen CJ, Watanabe K, Xiao ZC. 2003. F3/contactin acts as a functional ligand for Notch during oligodendrocyte maturation. Cell 115:163–175. https://doi.org/10.1016/s0092-8674(03)00810-9.

46. Popov VL, Yu X, Walker DH. 2000. The 120 kDa outer membrane protein of Ehrlichia chaffeensis: preferential expression on dense-core cells and gene expression in Escherichia coli associated with attachment and entry. Microb Pathog 28:71–80. https://doi.org/10.1006/mpat.1999.0327.

47. Ijdo JW, Carlson AC, Kennedy EL. 2007. *Anaplasma phagocytophilum* AnkA is tyrosine-phosphorylated at EPIYA motifs and recruits SHP-1 during early infection. Cell Microbiol 9:1284–1296. https://doi.org/10.1111/j.1462-5822.2006.00871.x.

48. Habyarimana F, Price CT, Santic M, Al-Khodor S, Kwaik YA. 2010. Molecular characterization of the Dot/Icm-translocated AnkH and AnkJ eukaryotic-like effectors of Legionella pneumophila. Infect Immun 78:1123–1134. https://doi.org/10.1128/IAI.00913-09.

49. Huang L, Boyd D, Amyot WM, Hempstead AD, Luo ZQ, O'Connor TJ, Chen C, Machner M, Montminy T, Isberg RR. 2011. The E Block motif is associated with Legionella pneumophila translocated substrates. Cell Microbiol 13:227–245. https://doi.org/10.1111/j.1462-5822.2010.01531.x.

50. Gomez-Valero L, Rusniok C, Cazalet C, Buchrieser C. 2011. Comparative and functional genomics of legionella identified eukaryotic like proteins as key players in host-pathogen interactions. Front Microbiol 2:208. https://doi.org/10.3389/fmicb.2011.00208.

51. Ravi Chandra B, Gowthaman R, Akhouri RR, Gupta D, Sharma A. 2004. Distribution of proline-rich (PxxP) motifs in distinct proteomes: functional and therapeutic implications for malaria and tuberculosis. Protein Eng Des Sel 17:175–182. https://doi.org/10.1093/protein/gzh024.

52. Klein T, Brennan K, Arias AM. 1997. An intrinsic dominant negative activity of serrate that is modulated during wing development in Drosophila. Dev Biol 189:123–134. https://doi.org/10.1006/dbio.1997.8564.

53. Semenova D, Bogdanova M, Kostina A, Golovkin A, Kostareva A, Malashicheva A. 2020. Dose-dependent mechanism of Notch action in promoting osteogenic differentiation of mesenchymal stem cells. Cell Tissue Res 379:169–179. https://doi.org/10.1007/s00441-019-03130-7.

54. Gomez-Lamarca MJ, Falo-Sanjuan J, Stojnic R, Abdul Rehman S, Muresan L, Jones ML, Pillidge Z, Cerda-Moya G, Yuan Z, Baloul S, Valenti P, Bystricky K, Payre F, O'Holleran K, Kovall R, Bray SJ. 2018. Activation of the Notch Signaling Pathway In Vivo Elicits Changes in CSL Nuclear Dynamics. Dev Cell 44: 611–623.e7. https://doi.org/10.1016/j.devcel.2018.01.020.

55. Cornell M, Evans DA, Mann R, Fostier M, Flasza M, Monthatong M, Artavanis-Tsakonas S, Baron M. 1999. The Drosophila melanogaster Suppressor of deltex gene, a regulator of the Notch receptor signaling pathway, is an E3 class ubiquitin ligase. Genetics 152:567–576. https://doi.org/10.1093/genetics/152.2.567.

56. Hambleton S, Valeyev NV, Muranyi A, Knott V, Werner JM, McMichael AJ, Handford PA, Downing AK. 2004. Structural and functional properties of the human notch-1 ligand binding region. Structure 12:2173–2183. https://doi.org/10.1016/j.str.2004.09.012.

57. Maveyraud L, Mourey L. 2020. Protein X-ray crystallography and drug discovery. Molecules 25:1030. https://doi.org/10.3390/molecules25051030.

58. Luo T, Zhang X, McBride JW. 2009. Major species-specific antibody epitopes of the *Ehrlichia chaffeensis* p120 and E. canis p140 orthologs in surface-exposed tandem repeat regions. Clin Vaccine Immunol 16:982–990. https://doi.org/10.1128/CVI.00048-09.

59. Veljkovic V, Vergara-Alert J, Segales J, Paessler S. 2020. Use of the informational spectrum methodology for rapid biological analysis of the novel coronavirus 2019-nCoV: prediction of potential receptor, natural reservoir, tropism and therapeutic/vaccine target. F1000Res 9:52. https://doi.org/10.12688/f1000research.22149.4.

60. Deng SP, Huang DS. 2014. SFAPS: an R package for structure/function analysis of protein sequences based on informational spectrum method. Methods 69:207–212. https://doi.org/10.1016/j.ymeth.2014.08.004.

61. Doyle CK, Nethery KA, Popov VL, McBride JW. 2006. Differentially expressed and secreted major immunoreactive protein orthologs of *Ehrlichia canis* and *E. chaffeensis* elicit early antibody responses to epitopes on glycosylated tandem repeats. Infect Immun 74:711–720. https://doi.org/10.1128/IAI.74.1.711-720.2006.

62. Luo T, Zhang X, Wakeel A, Popov VL, McBride JW. 2008. A variable-length PCR target protein of *Ehrlichia chaffeensis* contains major species-specific antibody epitopes in acidic serine-rich tandem repeats. Infect Immun 76: 1572–1580. https://doi.org/10.1128/IAI.01466-07.